Journal of Molecular Liquids 162 (2011) 129–134

Contents lists available at ScienceDirect

Journal of Molecular Liquids

journal homepage: www.elsevier.com/locate/molliq

Spectroscopic studies of the hydrogen bonded charge transfer complex of 2-aminopyridine with π-acceptor chloranilic acid in different polar solvents

Khairia M. Al-Ahmary [a], Moustafa M. Habeeb [b,*], Eman A. Al-Solmy [a]

[a] Chemistry Department, Faculty of Science, King Abdul-Aziz University, Jeddah, Saudi Arabia
[b] Chemistry Department, Faculty of Education, Alexandria University, Alexandria, Egypt

ARTICLE INFO

Article history:
Received 26 March 2011
Received in revised form 9 June 2011
Accepted 26 June 2011
Available online 19 July 2011

Keywords:
2-Aminopyridine
Chloranilic acid
UV–vis
FTIR

ABSTRACT

Hydrogen bonded charge transfer complex (HBCT) between 2-aminopyridine (2AP) as electron donor, hydrogen bond acceptor, with chloranilic acid (CHA) as the π-electron acceptor, hydrogen bond donor, has been studied spectrophotometrically in the polar solvents acetonitrile (AN), methanol (MeOH) and ethanol (EtOH). The stoichiometry of the complex has been identified by Job's and photometric titration methods to be 1:1. The Benesi–Hildebrand equation has been applied to estimate the formation constant (K_{CT}) and molar extinction coefficient (ε). It was found that the value of K_{CT} is larger in methanol than those in acetonitrile or ethanol. The results were interpreted in terms of Kamlet–Taft α and β solvent parameters. Furthermore, the data were analyzed in terms of standard free energy change (ΔG°), oscillator strength (*f*), dissociation energy (W), transition dipole moment (μ) and ionization potential (I_P). Also, the solid HBCT-complex was synthesized and characterized by using elemental analysis and FTIR spectroscopy.

1. Introduction

Proton or electron transfer complexes play an important role in the field of magnetic, electrical conductivity and optical properties [1–5]. A great number of charge transfer receptors have been reported under the basic construction strategy of employing hydrogen bonding [6–8]. Recent investigations have shown that hydrogen bonds could work as efficient bridges to mediate electron transfer between bonded species and initiate the so-called proton coupled electron transfer [9–12].

Generally, CT-interaction between benzoquinones electron acceptors and electron donors containing nitrogen, oxygen or sulfur atoms has been reported over the last years.

These types of interactions play an important role in the field of drug-receptors binding mechanism [13,14], surface chemistry [15], applications in solar energy storage [16], uses as organic superconductors [17], and in many biological fields as antibacterial and antifungal agents [18–20].

Aminopyridines are bioactive N-heterocyclic amines, which increase the strength of the nerve signal by blocking of the voltage-dependent K^+ channel [21,22]. Also, aminopyridines have been proposed as drugs for the treatment of many diseases such as myocardial infarction as antithrombus agents and diarrhea as antimicrobial agents [23–25]. In particular, 2-aminopyridine is one of the potential impurities in piroxicam and teroxicam which are non-steroided antiflammatory drugs that used in musculo-skeletal and joint disorders [26]. Moreover, aminopyridines are commonly present in synthetic and natural products [27]. They form repeated moiety in many large molecules with interesting photophysical, electrochemical and catalytic applications [28].

In connection with our work on electron or proton transfer complexes [29–34], and due to the biological and pharmaceutical applications of aminopyridines, this article presents our results on spectroscopic studies of the hydrogen bonded charge transfer complex between 2-aminopyridine with chloranilic acid (Scheme 1) in the different polar solvents acetonitrile, methanol and ethanol. The molecular composition of the complex was studied using Job's and photometric titration methods. The formation constant (K_{CT}), molar extinction coefficient (ε), standard free energy change (ΔG°), oscillator strength (*f*), transition dipole moment (μ), ionization potential (I_P) and dissociation energy (W) of the formed HBCT-complex were estimated and evaluated. In addition, the solid HBCT-complex was isolated and characterized using elemental analyses and infrared measurements.

2. Experimental

2.1. Physical measurements and chemicals

2.1.1. Electronic spectra

The electronic spectra were recorded in the region 700–250 nm using UV–vis Shimadzu UV-1601 spectrophotometer connected to Shimadzu TCC-ZUOA temperature controller unit (Japan).

* Corresponding author.
E-mail address: mostafah2002@yahoo.com (M.M. Habeeb).

0167-7322/$ – see front matter © 2011 Elsevier B.V. All rights reserved.
doi:10.1016/j.molliq.2011.06.015

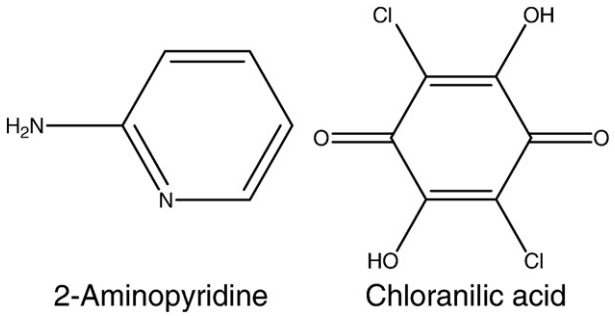

Scheme 1. Chemical structures of 2AP and CHA.

2.1.2. Infrared spectra

The infrared spectra were recorded as KBr disks on Bruker FTIR-Tensor 37 Fourier transform infrared spectrophotometer (USA), evacuated to avoid water and CO_2 absorption.

2.1.3. Elemental analyses

C, H and N contents were determined with the Micro analyzer Perkin Elmer 2400 (USA).

2.1.4. Chemicals

All chemicals used were of analytical grade. 2-aminopyridine was supplied by Acros Organics, chloranilic acid was supplied by Fluka. Acetonitrile, methanol and ethanol were purchased from PAI-ACS. KBr was spectroscopic grade supplied by Aldrich.

2.2. Synthesis of the solid 1:1 HBCT-complex

The solid HBCT-complex (1:1) between 2AP and CHA was prepared by mixing equimolar amounts of 2AP with CHA in acetonitrile. The resulting complex solution was allowed to evaporate slowly at room temperature where the complex was isolated as pink crystals. The separated complex was filtered off, washed well with acetonirile and dried over calcium chloride for 24 h. Anal. Calc. for (2AP-CHA) $C_{11}H_8N_2Cl_2O_4$ complex: C, 43.59%; H, 2.64%; N, 9.24%. Found: C, 43.64%; H, 3.05%; N, 9.29%. MP. 207–209 °C.

3. Results and discussion

3.1. Electronic spectra

Fig. 1 shows the electronic absorption spectra of 2AP, CHA and HBCT-complex in ethanol. While none of the reactants spectra

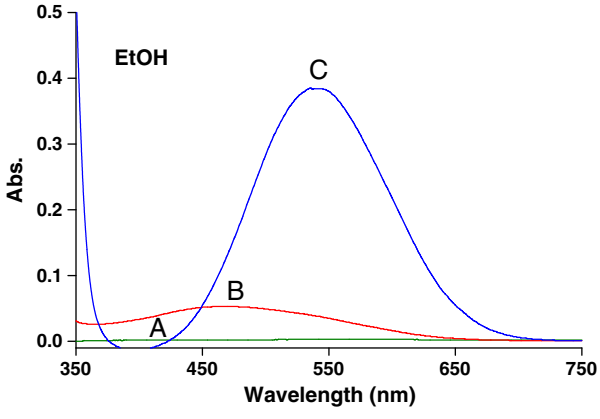

Fig. 1. Electronic spectra: (A) 2×10^{-4} M (2AP), (B) 2×10^{-4} M (CHA) and (C) [5×10^{-4} M (2AP) + 5×10^{-4} M (CHA)] in ethanol.

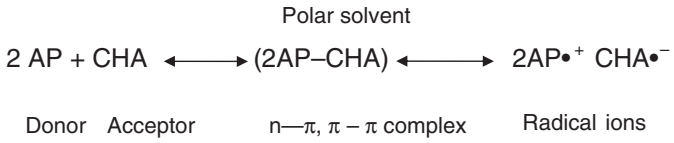

Scheme 2. Formation of CHA radical anion.

displays any measurable absorption in the region 450–600 nm, the resulting HBCT-complex shows strong absorption band centered at 519, 530 and 541 nm in AN, MeOH and EtOH, respectively. These absorptions are associated with the strong change in color observed upon mixing of the reactants (pink from colorless solutions in the different polar solvents). These reflect the electronic transitions in the formed HBCT-complex. It is important to report that the π-electronic spectra were scanned against the same electronic acceptor concentration to eliminate the possible overlap that may arise between HBCT-complex and CHA bands. Moreover, it is worth mentioning that the formed new long wave length absorption bands are attributed to the formation of CHA radical anion resulting from complete transfer of charge from 2AP to CHA (Scheme 2). The radical anion nature of benzoquinones has been confirmed by electron spin-resonance spectral measurements [35].

3.2. Effect of CHA concentration, reaction time and temperature on HBCT complex formation

The effect of CHA concentration was studied by following the absorbance of the HBCT-complex between varied amounts of 5×10^{-3} M CHA with 1 mL of 2×10^{-3} M 2AP in 10 mL calibrated flasks and diluted to the mark with solvent. It has been found that maximum constant absorbance of the HBCT-complex was obtained with 1 mL of 5×10^{-3} M CHA. The higher concentration of CHA causes negligible increase in absorbance. On the other hand, higher concentration of CHA may be useful to facilitate completion of the HBCT-complex that leads to minimize the required time for retaining the maximum absorbance at the corresponding wavelength.

The effect of time on the HBCT-reaction was studied by following the effect of time on the HBCT-complex produced by mixing 2×10^{-4} M from each of 2AN and CHA in the different solvents. It has been found that the absorbance of the HBCT-complex reached maximum and constant value instantly in the different solvents confirming that the time has no effect on the complex absorbance. In addition, the formed HBCT-complex was stable for 2 h (Table 1).

The effect of temperature was monitored by following the absorbance of the HBCT-complex resulting by mixing 5×10^{-4} M CHA with different concentrations of 2AP at different temperatures (20–40 °C). It has been found that the formed HBCT-complex was stable in the selected range at different 2AP concentrations as can be understood from its constant absorbance at different temperatures (Fig. 2). It seems that the extra stability of the formed complex through hydrogen bonding is presumably attributed to its high stability in the selected temperature range.

Table 1
Effect of time on the absorbance of 1:1 HBCT-complex.

Absorbance			
Time	AN	MeOH	EtOH
0	0.342	0.224	0.265
20	0.341	0.223	0.263
40	0.339	0.222	0.262
60	0.338	0.221	0.259
80	0.336	0.219	0.257
100	0.336	0.218	0.255
120	0.331	0.218	0.252

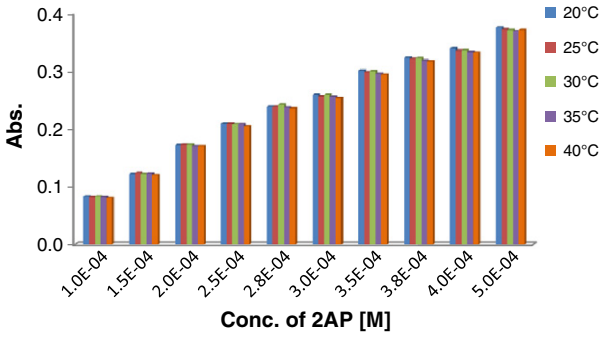

Fig. 2. Effect of temperature on the absorbance of HBCT-complex at different concentrations of 2AP in methanol.

3.3. Stoichiometric ratio of the formed HBCT-complex

The composition of the formed HBCT-complex was determined by applying Job's method of continuous variations [36] and photometric titrations [37]. Fig. 3 represents the continuous variation plot where maximum absorbance was recorded at 0.5 mol fraction indicating 1:1 HBCT-complex formation (2AP:CHA). Fig. 4 represents the photometric titrations where two straight lines were produced intercepting at 1:1 ratio (2AP: CHA). Accordingly, one can conclude from Figs. 3 and 4 that the HBCT-complex is formed based on a 1:1 stoichiometric ratio (2AP: CHA).

3.4. Formation constant of HBCT-complex

Based on the electronic spectra of the HBCT-complex at various 2AP concentrations, K_{CT} and ε were calculated using the modified Benesi–Hildebrand equation [38]

$$C^{\circ}_{d}C^{\circ}_{a}/A = 1/K_{CT}\varepsilon + (C^{\circ}_{d} + C^{\circ}_{a})/\varepsilon \quad (1)$$

where C°_{d} and C°_{a} are the initial concentrations of the electron donor and electron acceptor, respectively, and A is the absorbance of the CT-band. It is worth to mention that the maximum added 2AP concentration is approximately equal to the concentration of CHA and the calculated equilibrium constants are subjected to significant systematic errors due to the method used. Furthermore, the excess of 2AP concentration led to a decrease in the complex absorbance. This situation could be interpreted based on the high interaction between 2AP (pKa = 6.68) and solvents or the association of 2AP molecules through hydrogen bonding. These produce high steric hindrance leading to destabilizing the formed complex.

Plotting $C^{\circ}_{d}C^{\circ}_{a}/A$ versus $(C^{\circ}_{d} + C^{\circ}_{a})$ for the formed HBCT-complex in the different solvents, straight lines were obtained supporting our finding of the formation of 1:1 complex (Fig. 5). In the plots, the slope and intercept equal $1/\varepsilon$ and $1/\varepsilon K_{CT}$, respectively. The solvent parameters and the values of K_{CT}, ε and $\lambda_{max.}$ are compiled in Table 2.

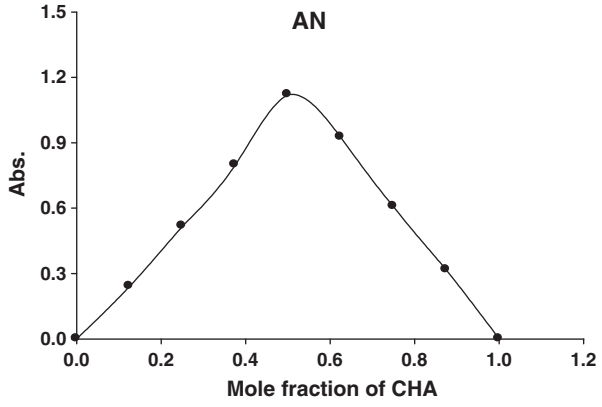

Fig. 3. Job's plots of HBCT-complex in acetonitrile.

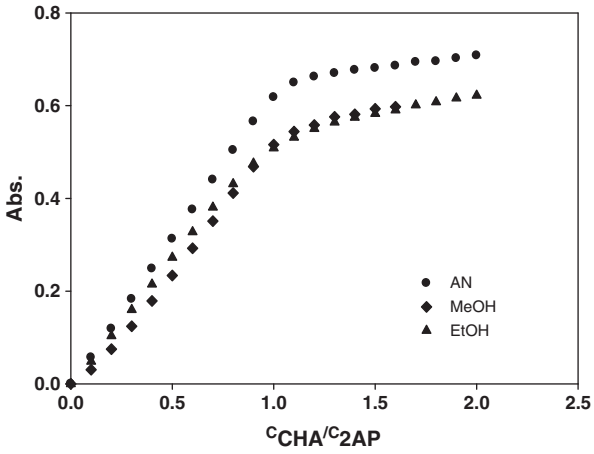

Fig. 4. Photometric titration plots of HBCT-complex in different solvents.

An important finding from Table 2 is the highest value of K_{CT} in methanol compared with those in acetonitrile or ethanol. This result could be interpreted based on the high value of the hydrogen bond donor parameter α of methanol, 0.98 [39]. This leads to solvation of CHA through hydrogen bond formation between methanol OH and the carbonyl groups of CHA. This increases the electronic accepting ability of CHA and hence K_{CT} increases. The small value of K_{CT} in acetonitrile could be explained in terms of its high value of the polarizability parameter π^{*}, 0.75 [39]. Consequently, acetonitrile molecules can form a dimer through self association owing to strong dipole–dipole interaction between these molecules leading to a small effective dipole moment and synergistic behavior that decreases K_{CT}. It is also observed in Table 2, the smallest value of K_{CT} in ethanol which could be rationalized based on the similar values of the hydrogen bond donor and acceptor parameters (α and β) 0.83 and 0.77 of ethanol [40]. Hence, ethanol molecules exhibit dual functions through solvation of both CHA and 2AP by hydrogen bonding interactions. The situation produces high steric hindrance leading to the smallest value of K_{CT} in ethanol.

3.5. Calculation of the oscillator strength and the transition dipole moment

The oscillator strength (f) is a dimensionless quantity which used to express the transition probability of the CT-band [41] and the transition dipole moment (μ) of the HBCT-complex [42]. The

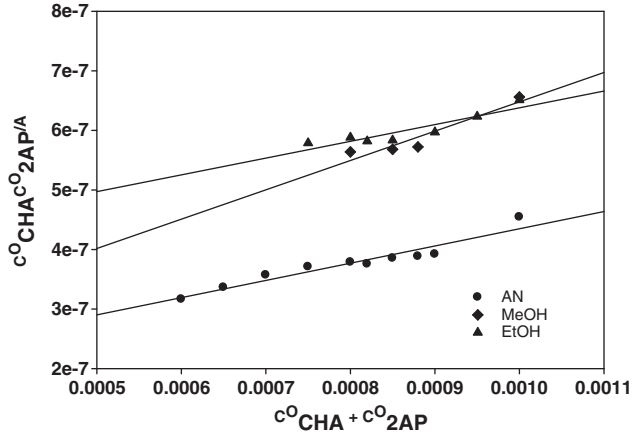

Fig. 5. Benesi–Hildebrand plots of 1:1 HBCT-complex in different solvents.

Table 2
Solvent parameters, Formation constant, molar extinction coefficient and wavelength of 1:1 HBCT-complex in different solvents.

Solvent	α	β	Π*	$K_{CT}\times10^{-3}$	$\varepsilon\times10^{-3}$	λ_{max}
				L mol^{-1}	L mol^{-1} cm^{-1}	nm
AN	0.19	0.31	0.75	1.99	3.46	519
MeOH	0.98	0.62	0.6	3.17	2.03	530
EtOH	0.83	0.77	0.54	0.79	3.55	541

following expressions [43] are commonly used to calculate *f* and μ. The results are compiled in Table 3.

$$f = 4.32\times10^{-9}\left[\varepsilon_{max}.\Delta\nu_{1/2}\right] \quad (2)$$

$$\mu = 0.0958\left[\varepsilon_{max}.\Delta\nu_{1/2}/\nu_{max}.\right]^{1/2} \quad (3)$$

where $\Delta\nu_{1/2}$ is the half band width of absorbance, $\varepsilon_{max.}$ and $\nu_{max.}$ are the molar extinction coefficient and wave number at the maximum absorption of the complex, respectively.

3.6. Calculation of the standard free energy change and dissociation energy

The standard free energy change of complexation (ΔG°) was calculated from the formation constant (K_{CT}) according to the following equation [44]

$$\Delta G^{\circ} = -2.303RT\ \log K_{CT} \quad (4)$$

where ΔG° is the free energy change of the complex (kJ mol^{-1}), R the gas constant (8.314 J mol^{-1} K), T is the absolute temperature (273 + °C) and K_{CT} is the formation constant of the HBCT-complex at 25 °C.

The dissociation energy (W) of the formed HBCT-complex was calculated from the corresponding CT energy (E_{CT}), ionization potential of the donor (I_P) and electron affinity of the acceptor (E_A) using the relationship [45]

$$E_{CT} = I_P - E_A - W. \quad (5)$$

The energy of the π–π* interaction (E_{CT}) is calculated using the following equation [46]

$$E_{CT} = 1243.667/\lambda_{CT}\text{nm} \quad (6)$$

whereas, λ_{CT} is the wavelength of the CT-band of the formed complex. The ionization potential values of the donors are calculated by using Eq. (7)

$$I_P = a + b(h\nu_{max.}) \quad (7)$$

where $h\nu_{max.}$ is the π–π* transition energy in electron volts eV, a and b are 5.11 and 0.701 [47], 4.39 and 0.857 [48] or 5.156 and 0.778 [49],

Table 3
Energy, ionization potential, dissociation energy, frees energy, oscillator strength and transition dipole moment of 1:1 HBCT-complex in different solvents.

Solvent	E_{CT} (eV)	I_P (eV)	W (eV)	−ΔG° (K.J.mol^{-1})	f	μ (Debye)
AN	2.40	8.00	4.50	18.79	0.73	8.98
MeOH	2.34	7.94	4.50	19.95	0.47	7.28
EtOH	2.30	7.90	4.50	16.51	0.47	7.38

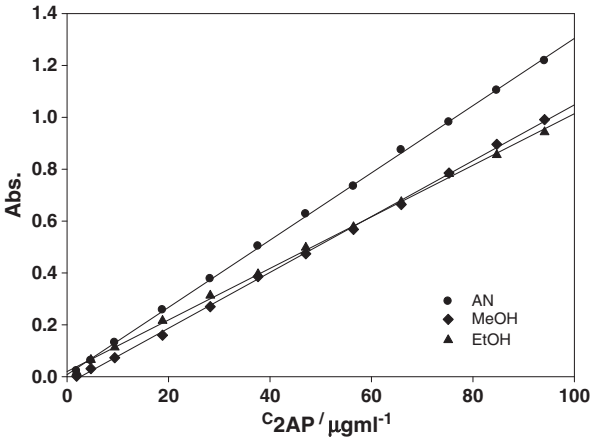

Fig. 6. Beer's law curves of 1:1 HBCT-complex in different solvents.

respectively, and the E_A of CHA is 1.1 eV [45]. E_{CT}, mean values of I_P, ΔG° and W are collected in Table 3.

It is evident from Table 3 that the formed HBCT-complex is characterized by relatively high values of both the oscillator strength and transition dipole moment. This confirms the charge transfer from 2AP to CHA to form the pink colored free radical anion of CHA.

The data in Table 3 clearly refer that the ionization potentials of the formed HBCT-complex are the same in the different solvents, confirming same overlapping molecular orbital between 2AP with CHA. In addition, the I_P has no effect on the stability of the formed HBCT-complex.

The calculated values of the dissociation energy (W) of the HBCT-complex in the different solvents are constant suggesting that the investigated complex is reasonably strong and stable under the studied conditions with high resonance stabilizing energy [50].

Furthermore, the negative values of the free energy change (ΔG°) listed in Table 2 suggest the simultaneous production of the formed HBCT-complex. Generally, the values of ΔG° given in Table 3 become more negative as the value of K_{CT} increases. As the bond between the donor and acceptor becomes stronger and thus the components are subjected to more physical strain or loss freedom, the values of ΔG° become more negative.

3.7. Application of the studied HBCT-reaction

Based on the formation of colored HBCT-complex between 2AP and CHA in the studied polar solvents, we propose in this section a

Table 4
Quantitative parameters of 1:1 HBCT-complex in different solvents.

Parameter	AN	MeOH	EtOH
Beer's law limits, μg mL^{-1}	1.88–94.12	1.88–94.12	1.88–94.12
Limit of detection, μg mL^{-1}	0.52	0.86	0.68
Limit of quantification, μg mL^{-1}	1.75	2.86	2.28
Regression equation	Y* = 0.0130X + 0.0079	Y* = 0.0108X − 0.0286	Y* = 0.0099X + 0.0199
Intercept, a	0.0079	−0.0286	0.0199
Slope, b	0.0130	0.0108	0.0099
Confidence interval of intercept, α	0.0079 ± 0.0011	−0.0286 ± 0.0015	0.0199 ± 0.0015
Confidence interval of slope, β	0.0130 ± 7.4×10^{-5}	0.0108 ± 0.0001	0.0099 ± 0.0001
Correlation coefficient, R^2	0.9997	0.9991	0.9989

* Y is the absorbance and X is the concentration in μ_g mL^{-1}.

Table 5
Precision and accuracy.

Solvent	Amount taken μg mL^{-1}	Amount found μg mL^{-1}	Rec. %	$\overline{X}$	SD	RSD	$\lvert\overline{X}-\mu\rvert$	$\pm\frac{tS}{\sqrt{n}}$	Confidence limits
AN	23.53	23.31	99.07	99.97	1.2275	1.2278	0.03	±1.41	99.97 ± 1.41
	32.94	32.96	100.04						
	51.77	52.79	101.97						
	70.59	70.53	99.92						
	80.00	79.10	98.87						
MeOH	14.12	14.46	102.44	100.31	3.56	3.55	0.31	±4.42	100.31 ± 4.42
	32.94	31.84	96.66						
	42.35	40.76	96.25						
	70.59	72.36	102.51						
	80.00	82.95	103.69						
EtOH	32.94	33.51	101.72	100.94	1.42	1.40	0.94	±1.76	100.94 ± 1.76
	42.35	42.56	100.49						
	51.77	53.13	102.63						
	61.18	61.78	100.98						
	80.00	79.08	98.85						

t = 2.776 for n = 5 at 95% confidence level.
SD = standard deviation.
RSD = relative standard deviation.

simple, rapid and accurate spectrophotometric method for determination of 2AP. Under the optimum reaction conditions Beer's plots at various 1:1 molar ratios between 2AP and CHA were constructed (Fig. 6). The regression equation in the different solvents was calculated by the least square method. In all cases Beer's law plots were linear with very small intercepts and slopes and good correlation coefficients in the general concentration range 2–94 μg ml^{-1} (Table 4). The limits of detection and quantification were calculated according to the IUPAC definition [51]. The calculated values were listed in Table 4. They recorded small values confirming high accuracy of the method. It has been found also that the values of the confidence intervals of intercept α, and slope β recorded small values confirming excellent linearity between the absorbance and concentration. The accuracy of the method was established by performing analysis of solutions containing five different amounts (within Beer's law limits) of 2AP and measuring the absorbance of their HBCT-complexes with CHA in different solvents. The concentration of 2AP was determined from the regression equation and then calculated the recovery percentages, the standard deviation S, and relative standard deviation RSD. The recovery percentage ranged from 99.71 to 100.94 with RSD ranging from 1.12 to 1.40 confirming high accuracy and precision of the proposed method (Table 5).

Comparison of the difference between the mean and true value ($X^- - \mu$) with the largest difference that could be expected as a result of indeterminate error ($\pm tS/\sqrt{n}$) [52] has been carried out and the results were collected in Table 5. It has been found that ($X^- - \mu$) were less than $\pm tS/\sqrt{n}$ indicating that no significant difference between the mean and true value is existed.

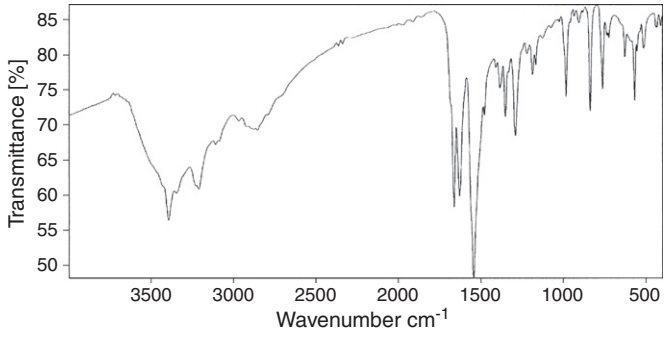

Fig. 7. FTIR spectrum of 1:1 HBCT-complex in the range 4000–400 cm^{-1}.

3.8. Infrared spectra

The formation of 1:1 HBCT-complex between 2AP and CHA was confirmed from a comparison of the infrared spectra of complex with those of 2AP or CHA. The infrared spectrum of the HBCT-complex is shown in Fig. 7 where the asymmetric and symmetric stretching vibrations of the amino group were weakened and shifted to 3393 and 3208 cm^{-1} compared with 3444 and 3290 cm^{-1} for 2AP. This confirms the formation of a hydrogen bonding between the amino group of 2AP and the OH of CHA. It is worth to mention that chloranilic acid is a dibasic acid ($pK_1 = 1.07$ and $pK_2 = 2.24$) [53,54], hence a proton transfer hydrogen bonding is expected to occur between the amino group and the more acidic OH of CHA. Returning to Fig. 7 one can observe a weak band at 2850 cm^{-1} which can be interpreted as due to $\nu(NH^+)$ stretching vibration. Consequently, the formed charge transfer complex is extra stabilized through bifurcated hydrogen bonding as shown in Scheme 3. The formation of the HBCT-complex is further confirmed from the shifts of its vibrational bands compared with 2AP and CHA. The carbonyl stretching vibrational band ν(C═O) is shifted to 1665 cm^{-1} compared with 1661 cm^{-1} for CHA, also ν(C═C) for the complex is recorded at 1629 cm^{-1} compared with 1627 cm^{-1} for 2AP. The recorded band at 1544 cm^{-1} in Fig. 7 could be assigned to in-plane bending δ(OH) overlapping with ν(C═N) of 2AP moiety that found at 1595 cm^{-1} for 2AP. In addition, ν(C–Cl)

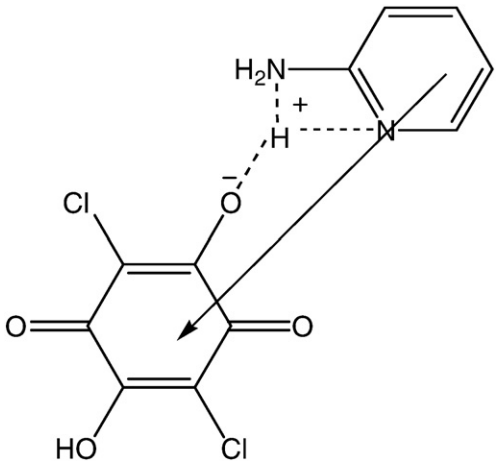

Scheme 3. Structure of crystalline HBCT-complex.

vibrational bands of the HBCT-complex were found at 838 and 761 cm^{-1} compared with 839 and 782 cm^{-1} for CHA. Furthermore, the ring vibrational bands at 576, 555, 513 cm^{-1} were further confirmed the formation of a bifurcated hydrogen bond in the HBCT-complex (2AP-CHA) [55,56].

4. Conclusion

1- 2AP reacts instantly with CHA to form HBCT-complex in different polar solvent.
2- Job's method of continuous variation and photometric titration methods confirmed the formation of 1:1 HBCT-complex.
3- K_{CT} of HBCT-complex in different polar solvents were estimated where K_{CT} recorded large value in methanol compared with ethanol and acetonitrile.
4- The results were interpreted based on Kamlet–Taft solvent parameters.
5- The solid HBCT-complex was isolated and characterized using elemental analysis and infrared spectroscopy.
6- The formed HBCT-complex included bifurcated hydrogen bonded proton transfer between OH of CHA and both the amino and ring nitrogen of 2AP.
7- Based on the simple composition of the formed HBCT-complex and its instantaneous production, a rapid and accurate spectrophotometric method for analysis of 2AP was suggested.
8- Beer's law was obeyed in the concentration range 2–94 μg ml^{-1}.
9- The recovery percentages ranged from 99.71 to 100.94 with relative standard deviation ranged from 1.12 to 1.40 confirming high accuracy and precision of the proposed method.

References

[1] A. Weller, K. Zachariasse, J. Chem. Phys. 46 (1967) 4904.
[2] R.K. Gupta, R.A. Sing, J. Appl. Sci. 5 (2005) 28.
[3] H.A. Hashem, M.S. Refat, Surf. Rev. Lett. 13 (2006).
[4] A. Tracz, Polym. J. Chem. 76 (2002) 457.
[5] I.M. Ishaat, A. Ahmed, Spectrochim. Acta A 77 (2010) 437.
[6] M.A. Hossain, J.M. Linares, D. Powell, K. Bouman-james, Inorg. Chem. 40 (2001) 2936.
[7] K.H. Lee, J.I. Hong, Tetrahedron Lett. 41 (2000) 6083.
[8] G. Hennrich, H. Sonnenschein, U. Reschgenger, Tetrahedron Lett. 42 (2001) 2805.
[9] I.V. Kuvykin, V.V. Ptushenko, A.V. Vershubskii, A.N. Tikhonov, Biochim. Biophys. Acta, Bioenerg. 1807 (2011) 336.
[10] H. Ozawa, T. Hino, H. Ohtsu, T. Wada, K. Tanaka, Inorg. Chim. Acta 366 (2011) 298.
[11] R. Vinu, S. Polisetti, G. Madras, Chem. Eng. J. 165 (2010) 784.
[12] C.J. Corcoran, H. Tavassol, M.A. Rigsby, P.S. Bagus, A. Wieckowski, J. Power Sources 195 (2010) 7856.
[13] A. Kololkovas, Essentials of Medicinal Chemistry, second ed. Wiley, New York, 1998 (Chapter 3).
[14] R. Mandal, S.C. Lahiri, J. Indian Chem. Soc. 76 (1999) 347.
[15] S.M. Andrade, S.M.B. Costa, R. Pansu, J. Colloid Interface Sci. 226 (2000) 260.
[16] K. Takahasi, K. Horino, T. Komura, K. Murata, Bull. Chem. Soc. Jpn. 66 (1993) 733.
[17] A. Eychmuller, A.I. Rogach, Pure Appl. Chem. 72 (2000) 179.
[18] H. Salem, J. Pharm. Biomed. Anal. 29 (2002) 527.
[19] A.M. Slifkin, Charge Transfer Interaction of Biomolecules, Academic Press, New York, 1971.
[20] L.B. Kiev, Molecular Orbital Theory in Drug Research, Academic Press, New York, 1971.
[21] J. Melgo, M. Lemeignan, F. Peradejordi, P. Lechat, J. Pharmacol. (Paris) 16 (Suppl. II) (1985) 109.
[22] C. Carlsoom, I. Rosen, E. Nilsson, Acta Anaesthesiol. Scand. 27 (1993) 87.
[23] J.I. Segal, B.S. Brunnemann, Pharmacotherapy 17 (1997) 415.
[24] A.G. Amr, A.M. Mohamed, S.F. Mohamed, N.A. Abdel-Hafez, A. Hammam, Bioorg. Med. Chem. 14 (2006) 5488.
[25] I.O. Zhuravel, S.M. Kovalenko, A.V. Ivachtchenko, K.V. Balakin, V. Kazmirchuk, Bioorg. Med. Chem. Lett. 5 (2005) 5483.
[26] K. Parfitt, S.C. Sweetman, P.S. Blake, A.V. Parsons, Martindale, The Extra Pharmacopoeia, 32nd ed, Phamaceutical Press, London, 1999, p. 80, 88.
[27] A. Goel, V.J. Ram, Tetrahedron 65 (2009) 7865.
[28] N.A. Al-Hashimy, Y.A. Hussein, Spectrochim. Acta A 75 (2010) 198.
[29] M.M. Habeeb, A.S. Al-Attas, M.T. Basha, J. Mol. Liq. 150 (2009) 56.
[30] M.M. Habeeb, R.M. Alghanmi, JCED 55 (2010) 930.
[31] K.M. Al-Ahmary, M.M. Habeeb, E.A. Al-Solmy, J. Solution Chem. 39 (2010) 1264.
[32] A.S. Al-Attas, M.M. Habeeb, D.S. Al-Raimi, J. Mol. Liq. 148 (2009) 58.
[33] A.S. Al-Attas, M.M. Habeeb, D.S. Al-Raimi, J. Mol. Struct. 928 (2009) 158.
[34] K.M. Al-Ahmary, M.M. Habeeb, E.A. Al-Solmy, J. Mol. Liq. 158 (2011) 161.
[35] M.E. Abdel-Hamid, M. Abdel-Salam, M.S. Mahrous, M.M. Abdel-Khalek, Talanta 32 (1985) 1000.
[36] P. Job, Advanced Physicochemical Experimental: London, , 1964.
[37] D.A. Skoog, Principal of Instrumental Analysis, 3rd ed. Sunder College Publisher, New York, 1985.
[38] H. Benesi, J. Hildebrand, J. Am. Chem. Soc. 71 (1949) 2703.
[39] N.S. Moyon, A.K. Chandra, S. Mitra, J. Phys. Chem. A114 (2010) 60.
[40] K.A. Connors, Chemical Kinetics, The Study of Reaction Rate in Solution, VCH Publishers, Inc, 1990.
[41] A.B.P. Leve, Inorganic Electronic Spectroscopy, second ed., Elsevier, Amsterdam, 1985, p. 161.
[42] H. Tsubomura, R. Lang, J. Am. Chem. Soc. 86 (1964) 3930.
[43] R. Rathone, S.V. Linderman, J.K. Kochi, J. Am. Chem. Soc. 119 (1997) 9393.
[44] W.B. Person, J. Am. Chem. Soc. 84 (1962) 536.
[45] H.M. McConnel, J.J. Ham, J.R. Platt, J. Chem. Phys. 21 (1964) 66.
[46] G. Briegleb, Z. Angew Chem. 76 (1964) 326.
[47] D.C. Wheat, Hand Book of Chemistry and Physics, fifteenth ed., CRC, 1969–1970.
[48] A.F. Mosten, J. Chem. Phys. 24 (1956) 602.
[49] S.R. Becker, F.W. Worth, J. Am. Chem. Soc. 84 (1962) 4263.
[50] M. Pandeeswaran, K.P. Elango, Spectrochim. Acta A 65 (2006) 1148.
[51] M.H. Irving, T.S. Freiser, West. IUPAC Compendium of Analytical Nomenclature Definitive Rules, Pergamon Press, Oxford, 1981.
[52] J.C. Miller, N.A. Miller, Statistics for Analytical Chemistry, second ed. Ellis Horwood Ltd, England, 1988.
[53] M.M. Habeeb, H.A. Alwakil, A. El-Dissouky, H. Abdel-Fattah, Pol. J. Chem. 69 (1995) 1428.
[54] G.H. Gohar, M.M. Habeeb, Spectroscopy 14 (2000) 99.
[55] J. Kalenik, I. Majerz, L. Sobczyk, E. Grech, M.M. Habeeb, J. Chem. Soc., Faraday Trans. 1 85 (1989) 3187.
[56] J. Kalenik, I. Majerz, L. Sobczyk, E. Grech, M.M. Habeeb, Collect. Czech. Chem. Commun. 55 (1990) 80.